Rare Metal Materials and Engineering
Volume 50, Issue 7, July 2021
Available online at www.rmme.ac.cn

Science Press

Cite this article as: Jiang Nan, Zhang Liang, Xu Kaikai, et al. Reliability of Graphene Nanosheets-Reinforced Sn-58Bi/Cu Solder Joints[J]. Rare Metal Materials and Engineering, 2021, 50(07): 2293-2299.

ARTICLE

Reliability of Graphene Nanosheets-Reinforced Sn-58Bi/Cu Solder Joints

Jiang Nan[1], Zhang Liang[1,2], Xu Kaikai[1], Wang Fengjiang[3], Long Weimin[4]

[1] School of Mechatronic Engineering, Jiangsu Normal University, Xuzhou 221116, China; [2] State Key Laboratory of Advanced Welding and Joining, Harbin Institute of Technology, Harbin 150001, China; [3] School of Materials Science and Engineering, Jiangsu University of Science and Technology, Zhenjiang 212000, China; [4] State Key Laboratory of Advanced Brazing Filler Metals & Technology, Zhengzhou Research Institute of Mechanical Engineering, Zhengzhou 450001, China

Abstract: Graphene nanosheets (GNSs) of different mass fractions (0wt%, 0.025wt%, 0.05wt%, 0.075wt%, 0.1wt%, and 0.2wt%) were added into the Sn-58Bi low-temperature solder. The influences of GNSs on melting characteristics, wettability, shear properties, microstructure and interfacial reaction were investigated. Results show that adding GNSs has the positive effect on the wettability and shear strength of Sn-58Bi solder joint, and a slight influence on the melting temperature. After the addition of GNSs, a finer microstructure of Sn-58Bi solder is obtained. The thickness of intermetallic compound (IMC) at solder/Cu interface reduces significantly and the IMC morphology becomes flat after adding GNSs. In addition, with the addition of GNSs, the shear fracture mode of Sn-58Bi low-temperature solder converts from brittle into a mixed mode of brittle and ductile fracture, which is coincident with the changing situation of shear strength. In general, adding GNSs may be conducive to the improvement of solder joint reliability.

Key words: graphene nanosheet; microstructure; wettability; shear strength; reliability

Owing to the good wettability and mechanical properties, SnPb solder has been extensively applied in the electronic packaging field[1,2]. However, with increasing the awareness of environmental protection, the application of SnPb solder is greatly restricted. Until now, many kinds of Pb-free solders have been considered as ideal substitute for SnPb solder, such as SnAgCu, SnCu, SnAg, SnBi, and SnZn solder[3,4], among which SnBi solder is widely used in low temperature soldering because of its relatively low cost and low melting point (139 °C)[5]. But the extensively practical application of SnBi solder is restricted because of the brittleness characteristic[6].

A feasible and effective method to improve the performance of SnBi solder is to introduce nanomaterials as reinforcements into the SnBi solder alloy[7]. Yang et al[8] added CuZnAl particles into Sn-58Bi solder, and found that the addition of CuZnAl particles can effectively increase the spreading area of the solder, thereby improving the wettability of the solder. Liu et al[9] reported that the addition of Cu nanoparticles refines the microstructure of the Sn-58Bi solder but has a negative influence on the wettability. The decrease of wettability may be attributed to the reduction of solder viscosity after adding the Cu nanoparticles[10]. Ma et al[11] studied the influence of addition of graphene nanosheets (GNSs) on the mechanical properties of SnBi solder. It is found that adding GNSs increases the hardness and tensile strength of SnBi solder after aging. Since adding GNSs can obtain a finer microstructure, the mechanical properties improve significantly on the basis of Hall-Petch mechanism[12]. Yang et al[13] fabricated Sn-58Bi composite solder by doping carbon nanotubes (CNTs), which effectively improves the tensile creep resistance of solder. The CNTs can offer more obstacles to dislocation pile-up, thereby improving the creep activation energy values and the stress exponent. Among these reinforcements, GNSs have important application prospect in the electronic packaging field because of their

Received date: July 11, 2020
Foundation item: Key Project of State Key Laboratory of Advanced Welding and Joining (AWJ-19Z04); National Natural Science Foundation of China (51475220); Six Talent Peaks Project in Jiangsu Province (XCL-022)
Corresponding author: Zhang Liang, Ph. D., Professor, School of Mechatronic Engineering, Jiangsu Normal University, Xuzhou 221116, P. R. China, E-mail: zhangliang@jsnu.edu.cn

superior thermal, electrical and mechanical properties[14]. Nevertheless, in the current study, there are few systematic researches on adding GNSs in SnBi solder, which restricts the wide application of this composite solder in electronic packaging.

In this research, the effects of GNSs addition on melting characteristics, wettability, microstructure, shear strength and interface reaction of Sn-58Bi low-temperature solder were studied. The shear fracture mechanism of solders was also investigated.

1 Experiment

The raw materials were GNSs powder and Sn-58Bi solder (50 nm). The Sn-58Bi composite solders were prepared by mechanical addition of 0wt%, 0.025wt%, 0.05wt%, 0.075wt%, 0.1wt% and 0.2wt% GNSs powder into the Sn-58Bi solder, and then fusion in a vacuum arc furnace at 600 °C for 60 min, namely Sn-58Bi-*x*GNSs with *x*=0, 0.025, 0.05, 0.075, 0.1, 0.2. Then the molten solder was chill-cast in a mold to form the solder ingots. Finally, small pieces were cut from the solder ingots and extruded into thin sheets via an electric tablet press (HY2-60). The morphologies and structure of raw materials and specimens were analyzed by scanning electron microscope (SEM) and X-ray diffraction (XRD), respectively. The dimension of GNSs raw powder is 1~5 μm, as shown in Fig. 1a. Some folds and wrinkles located on GNSs surface indicate that GNSs have the typical characteristics of 2D thin graphene. Fig.1b reveals the XRD pattern of GNSs powder. It can be seen that the reflection at 2θ=26° is the diffraction peak of GNSs, and the peak intensity is at 25.82°.

The melting characteristic is the basic performance and can directly determine the solderability of the solder[15]. The STA449 F3 differential scanning calorimeter (DSC) was applied to measure the melting temperature of alloys. The solder pieces of about 15 mg were placed in the Al_2O_3 crucible. The DSC samples were heated to 200 °C with a heating rate of 10 °C/min.

The wettability is one of the important standards for evaluating the solder performance[16]. The Cu substrates with the size of 25 mm×25 mm×0.3 mm were rinsed by ultrasonic cleaner in ethanol for 1 min. The solder pieces of 0.2 g were put on the Cu substrates separately and then heated to 180 °C in the T-962 reflow furnace.

The UTM5000 electronic universal testing machine was used in the shear experiment to determine the shear strength of solder joints. The schematic illustration of all samples is shown in Fig.2. The size of the coated solder is 3 mm×3 mm×0.3 mm. The dimension of Cu plates is 40 mm×4 mm×0.6 mm. Before the shear test, the Cu substrates were ground with sandpapers, and then rinsed by ultrasonic cleaner in ethanol for 1 min. The morphology of shear fracture was observed by SEM.

For the analysis of microstructure and interfacial intermetallic composite (IMC) layer, all samples were sectioned, and then embedded in the cold epoxy resin. The samples were ground by sandpapers and polished by diamond paste of 1.5 μm. In order to distinctly observe the morphology of interfacial IMC, the samples were corroded with 95vol% CH_3CH_2OH+5vol% HNO_3 solution for 1~3 s. The morphologies of IMC at the interface were observed by SEM. An energy dispersive spectroscopy (EDS) was used to determine the chemical composition of IMC. To further study the effect of adding GNSs on IMC of solder/Cu interface, the average thickness of IMC layer (χ) was calculated by Eq.(1):

$$\chi = \frac{A}{L} \quad (1)$$

where A is the area of the IMC layer, and L is the length of IMC layer in the interface.

2 Results and Discussion

2.1 Melting characteristics

Fig. 3 shows the DSC results and melting temperatures of different SnBi-*x*GNSs specimens. The solidus temperature (T_S) of the Sn-58Bi-*x*GNSs (*x*=0, 0.025, 0.05, 0.075, 0.1, 0.2) solder ranges from 138.25 °C to 138.73 °C. The liquidus temperature (T_L) of Sn-58Bi-*x*GNSs composites ranges from 139.49 °C to 140.56 °C. The result demonstrates that GNSs addition has little influence on the melting temperature of Sn-58Bi low-temperature solder alloys, because the melting point of solder alloy is an intrinsic physical property.

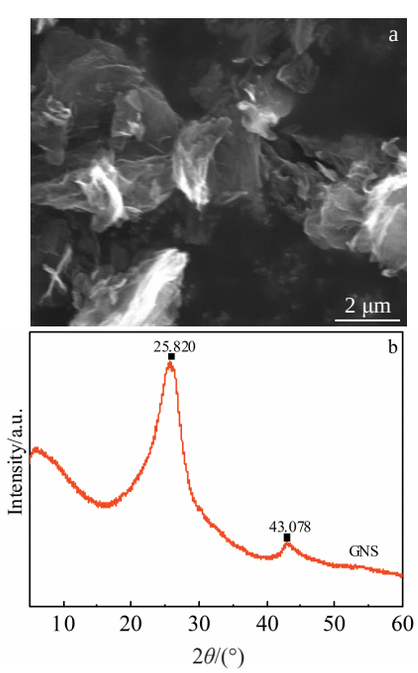

Fig.1 SEM image (a) and XRD pattern (b) of GNSs

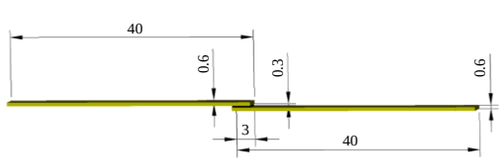

Fig.2 Schematic diagram of samples (unit: mm)

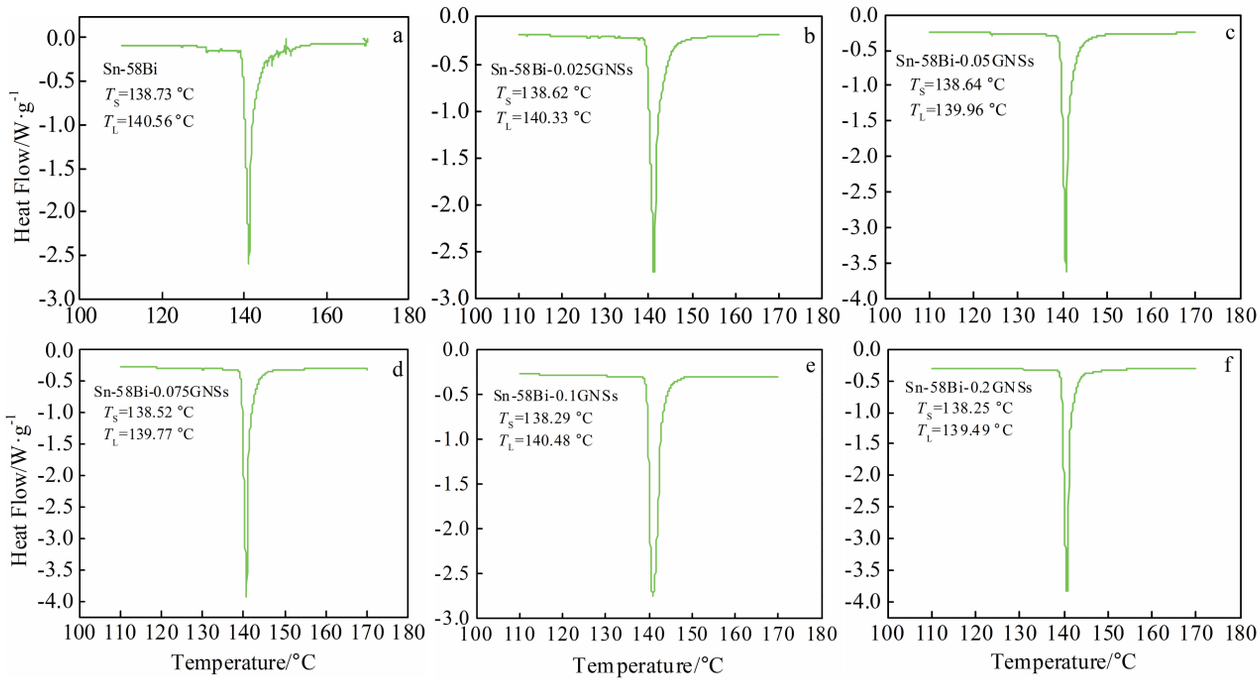

Fig.3 DSC curves of different SnBi-*x*GNSs solders: (a) *x*=0, (b) *x*=0.025, (c) *x*=0.05, (d) *x*=0.075, (e) *x*=0.1, and (f) *x*=0.2

2.2 Wettability

Fig. 4 presents the spreading area of the Sn-58Bi-*x*GNSs solders. It can be seen that the spreading area of Sn-58Bi solder is obviously smaller than that of solder after adding GNSs, indicating that the minor addition of GNSs improves significantly the wettability of the Sn-58Bi solder. It is well known that the capillary phenomenon also exists at the solder/Cu interface and is beneficial to the improvement of solder fluidity[17]. GNSs do not melt during the soldering process, but act as the reinforcing phase to strengthen the capillary phenomenon. In particular, the spreading area of Sn-58Bi-0.05GNSs solder rises to 84.1 mm^2, increasing by 23.3% compared to that of Sn-58Bi solder (68.2 mm^2). However, when the addition content of GNSs exceeds 0.05wt%, the spreading area of Sn-58Bi composite solder gradually decreases. The excess GNSs easily agglomerate on the solder surface[18,19], resulting in the decrease of the solder fluidity.

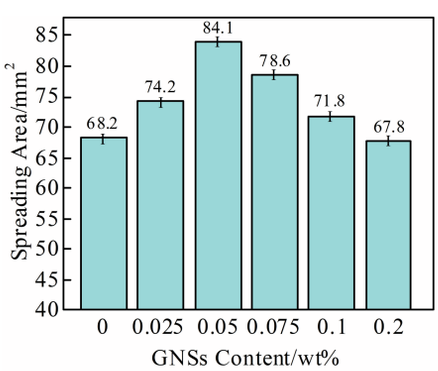

Fig.4 Spreading area of different Sn-58Bi-*x*GNSs solders

2.3 Mechanical properties

Fig.5 shows the shear strength of different Sn-58Bi-*x*GNSs solders. It is evident that the shear strength of solder joints with the addition of GNSs is better than that of Sn-58Bi solder, indicating that the addition of GNSs enhances the shear strength of solder joints because of the promotion of nucleation and grain refinement. The GNSs addition improves the mechanical properties on the basis of Hall-Petch mechanism[20]. In addition, GNSs act as the second particles and are distributed dispersively in the solder matrix. Based on Orowan mechanism, the dispersion strengthening can be expressed by Eq.(2):

$$\sigma_{org} = \frac{2Gb}{\lambda} \quad (2)$$

where σ_{org} refers to the yield stress, G is the shear modulus of solder matrix, b represents the Burger's vector of the dislocation, and λ refers to the distance between the dispersed GNSs. The yield stress of Sn-58Bi-*x*GNSs solders improves because λ decreases. In addition, the mechanical properties of solder joints depend generally on the bond strength between the solder alloys and substrates[21], suggesting that IMC is critical for the reliability of solder joints. Particularly, the brittleness of IMC may degrade the reliability of solder joints, whereas thin and continuous IMC layer can effectively enhance the reliability of solder joints[22]. Therefore, the improvement of shear strength may be attributed to the reduction of IMC.

Sn-58Bi solder joint with 0.075wt% GNSs presents the best shear strength among these solder joints. Nonetheless, the shear strength of solder joint gradually reduces as the GNSs

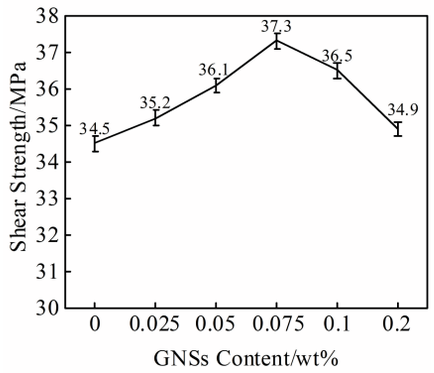

Fig.5 Shear strength of different Sn-58Bi-*x*GNSs solders

content further increases. The aggregations of GNSs weaken the function, acting as the nucleating particles. As a result, the excessive addition of GNSs reduces the shear strength of solder joints slightly.

The shear fractures reveal the shear properties of these specimens, as shown in Fig.6. Some grain contours are observed in Fig. 6a, indicating that the fracture mode of Sn-58Bi solder is the typical brittle fracture[23]. As shown in Fig.6b and 6c, the fracture surface shows slightly tearing markings. The plastic deformation occurs and a lot of tearing markings appear in Fig. 6d~6f[24]. Therefore, the fracture mode of Sn-58Bi solder converts from brittle to a mixed mode of brittle and ductile fracture. The results are coincident with the improvement of shear strength.

2.4 Microstructure

Fig. 7 reveals the SEM images of Sn-58Bi and the composite solders. With the GNSs addition, the grains of Sn-58Bi-*x*GNSs composite solders are refined, as shown in Fig. 7a~7d. It can be seen from Fig. 7d that the smaller Bi grains and relatively uniform microstructure appear in the Sn-58Bi-0.075GNSs composite solder, suggesting that adding GNSs restrains the grain growth, thereby refining the solder microstructure. Because GNSs act as the barrier which inhibits the diffusion of metal atoms, the growth of Cu_6Sn_5 grains is restricted[25].

Nonetheless, as the GNSs content increases from 0.075wt% to 0.2wt%, the microstructure of the Sn-58Bi-*x*GNSs composite solders slightly coarsens, as shown in Fig. 7d~7f. When GNSs are added in excess, the growth of metal grains along the GNSs surface can be promoted, resulting in the coarsening of solder microstructure.

2.5 Interfacial IMC layer

Fig. 8 exhibits the SEM images of Sn-58Bi-*x*GNSs composite solders/Cu interfaces. A scallop-shaped and continuous IMC layer forms at Sn-58Bi/Cu interface. The composition of interfacial IMC is shown in Fig. 9, indicating that IMC consists of Cu_6Sn_5 (57.39at% Cu and 42.61at% Sn). The morphology of the interfacial IMC layer markedly changes with the addition of the GNSs. When the addition amount of GNSs is 0.075wt%, IMC morphology becomes relatively flat, as shown in Fig. 8d. As GNSs content further increases, the interfacial IMC becomes uneven, as shown in Fig.8e and 8f.

The average thickness of interfacial IMC is shown in Fig.10. It is found that the interfacial IMC thickness decreases significantly as the addition amount of GNSs increases, suggesting that the GNSs addition suppresses the IMC growth. The mean thickness of IMC layer decreases linearly from 1.15 μm to 0.91 μm as the GNSs content increases from 0wt% to 0.075wt%, which may be related to the change of surface free energy caused by the adsorption properties of nanoparticles. Based on the adsorption theory, the surface free energy equation is given as follows[26]:

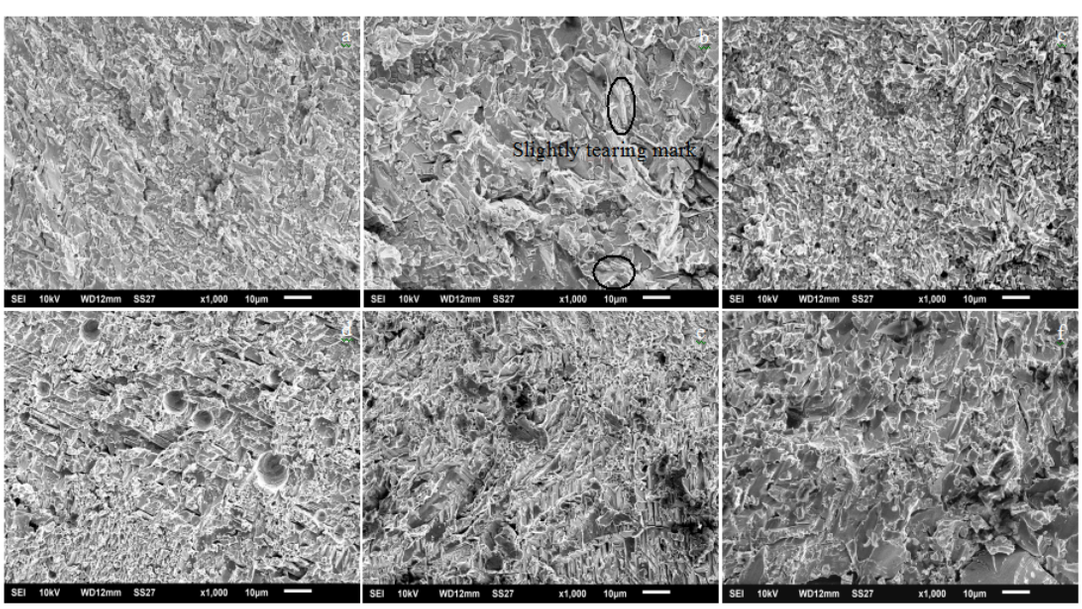

Fig.6 SEM images of shear fractures of different SnBi-*x*GNSs solders: (a) *x*=0, (b) *x*=0.025, (c) *x*=0.05, (d) *x*=0.075, (e) *x*=0.1, and (f) *x*=0.2

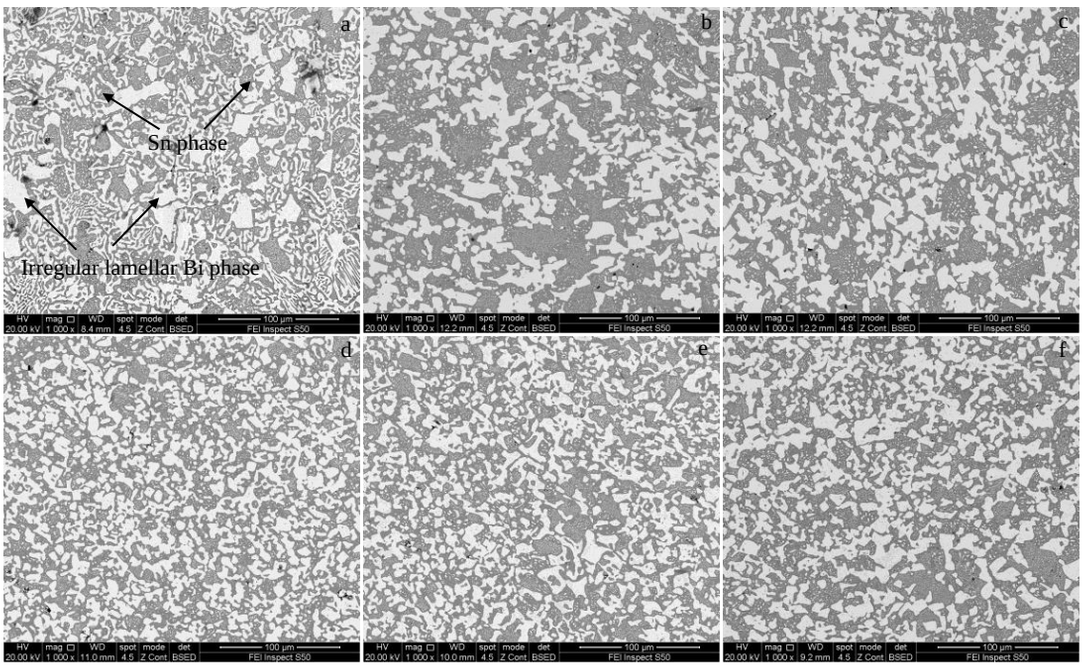

Fig.7 SEM images of microstructure in Sn-58Bi-*x*GNSs: (a) *x*=0, (b) *x*=0.025, (c) *x*=0.05, (d) *x*=0.075, (e) *x*=0.1, and (f) *x*=0.2

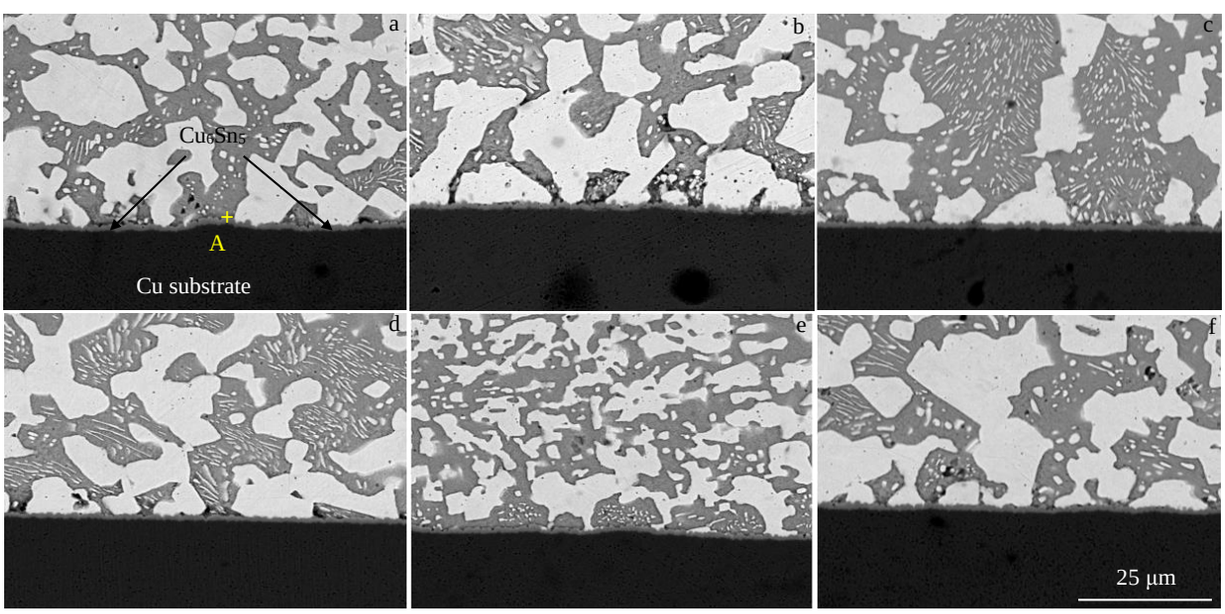

Fig.8 Interfacial IMC layers of Sn-58Bi-*x*GNSs/Cu solder joints: (a) *x*=0, (b) *x*=0.025, (c) *x*=0.05, (d) *x*=0.075, (e) *x*=0.1, and (f) *x*=0.2

$$\sum_K \gamma_c^K A_K = \sum_K \left(\gamma_0^K - RT \int_0^c \frac{\Gamma^K}{c} \mathrm{d}c \right) A_K \rightarrow \min \quad (3)$$

where γ_c^K represents the surface tension of Cu_6Sn_5 crystal plane K with adsorption of GNSs; R and T are the thermodynamic temperature and Planck constant, respectively; A_K is the area of crystal plane; c and Γ^K is the concentration and adsorption of GNSs at crystal plane K, respectively; γ_0^K represents the surface tension of crystal plane without adsorption of GNSs.

When $\sum_K A_K \int_0^c \frac{\Gamma^K}{c} \mathrm{d}c \rightarrow \max$, the free energy of the crystal is minimized. At the grain boundary of Cu_6Sn_5, the increase of GNSs surface-active material adsorption decreases the surface energy, thereby reducing the growth rate of the Cu_6Sn_5 IMC plane. However, the IMC thickness increases slightly with the further addition of GNSs. Because GNSs are diffused into the solder/Cu interface, the activation energy of Cu_6Sn_5 grain

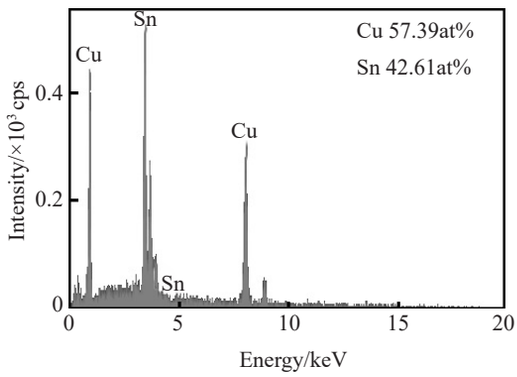

Fig.9 EDS spectrum of interfacial IMC (point A) in Fig.8a

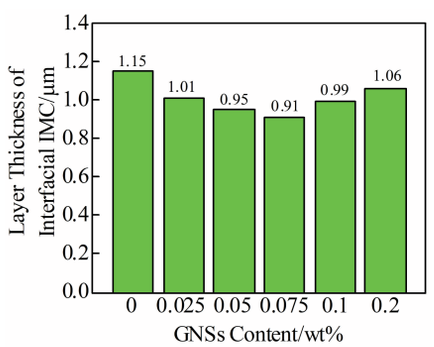

Fig.10 Layer thicknesses of interfacial IMC at different Sn-58Bi-*x*GNSs solder/Cu interfaces

boundary reduces, leading to the thickness decrease of the Cu_6Sn_5 IMC layer.

3 Conclusions

1) Graphene nanosheets (GNSs) addition improves the wetting behavior of Sn-58Bi low-temperature solder, but has slight influence on the melting temperature.

2) The shear strength of Sn-58Bi-GNSs composite solder joints improves, which is attributed to a the shear fracture mode change from brittle (Sn-58Bi) to a mixed mode of brittle and ductile fracture caused by the GNSs addition.

3) As the GNSs content increases, the microstructure of low-temperature Sn-58Bi-GNSs composite solders becomes finer, and the thickness of interfacial intermetallic composite (IMC) reduces (in a certain range). In addition, the IMC morphology becomes flat by adding GNSs.

References

1 Zhao M, Zhang L, Liu Z Q *et al*. *Science and Technology of Advanced Materials*[J], 2019, 20(1): 421

2 Jiang N, Zhang L, Liu Z Q *et al*. *Science and Technology of Advanced Materials*[J], 2019, 20(1): 876

3 Zhang Z, Hu X W, Jiang X X *et al*. *Metallurgical and Materials Transactions A*[J], 2019, 50: 480

4 Xiong M Y, Zhang L. *Journal of Materials Science*[J], 2019, 54(2): 1741

5 Wang F J, Huang Y, Zhang Z J *et al*. *Materials*[J], 2017, 10(8): 920

6 Wang F J, Chen H, Huang Y *et al*. *Journal of Materials Science, Materials in Electronics*[J], 2019, 30(4): 3222

7 El-Daly A A, Desoky W M, Elmosalami T A *et al*. *Materials & Design*[J], 2015, 65: 1196

8 Yang F, Zhang L, Liu Z Q *et al*. *Materials*[J], 2017, 10(5): 558

9 Liu Y, Zhang H, Sun F L. *Journal of Materials Science, Materials in Electronics*[J], 2016, 27(3): 2235

10 Zhang H, Liu Y, Sun F L *et al*. *Microelectronics International*[J], 2017, 34(1): 40

11 Ma Y, Li X, Yang L *et al*. *Materials Science and Engineering A* [J], 2017, 696: 437

12 Chuang T H, Tsao L C, Chung C H *et al*. *Materials & Design*[J], 2012, 39: 475

13 Yang L, Liu H, Zhang Y. *Journal of Electronic Materials*[J], 2018, 47(1): 662

14 Liu X D, Han Y D, Jing H Y *et al*. *Materials Science and Engineering A*[J], 2013, 562: 25

15 Fan J L, Zhai H T, Liu Z U *et al*. *Journal of Electronic Materials* [J], 2020, 49(4): 2660

16 Shen J, Pu Y, Yin H *et al*. *Journal of Electronic Materials*[J], 2015, 44(1): 532

17 Derrick A, Sachin S V. *Colloids and Surfaces A, Physicochemical and Engineering Aspects*[J], 2018, 553: 624

18 Jing H Y, Guo H J, Wang L X *et al*. *Journal of Alloys and Compounds*[J], 2017, 702: 669

19 Xu L Y, Wang L X, Jing H Y *et al*. *Journal of Alloys and Compounds*[J], 2015, 650: 475

20 Sun L, Chen M H, Wei C C *et al*. *Journal of Materials Science, Materials in Electronics*[J], 2018, 29(12): 9757

21 Gao H, Wei F X, Sui Y W *et al*. *Journal of Materials Science, Materials in Electronics*[J], 2019, 30(3): 2186

22 Xiong M Y, Zhang L, Sun L *et al*. *Vacuum*[J], 2019, 167: 301

23 Zhu W B, Zhang W W, Zhou W *et al*. *Journal of Alloys and Compounds*[J], 2019, 789: 805

24 Silva B L, Xavier M G C, Garcia A *et al*. *Materials Science & Engineering A*[J], 2017, 705: 325

25 Gan Y, Sun L, Banhart F. *Small*[J], 2008, 4(5): 587

26 Jiang N, Zhang L, Liu Z Q *et al*. *Journal of Materials Science: Materials in Electronics*[J], 2019, 30(19): 17 583

石墨烯纳米片增强的Sn-58Bi/Cu焊点可靠性

姜　楠[1]，张　亮[1,2]，徐恺恺[1]，王凤江[3]，龙伟民[4]

(1. 江苏师范大学 机电工程学院，江苏 徐州 221116)

(2. 哈尔滨工业大学 先进焊接与连接国家重点实验室，黑龙江 哈尔滨 150001)

(3. 江苏科技大学 材料科学及工程学院，江苏 镇江 212000)

(4. 郑州机械研究所 新型钎焊材料与技术国家重点实验室，河南 郑州 450001)

摘　要：将不同含量（0%，0.025%，0.05%，0.075%，0.1%，0.2%，质量分数）的石墨烯纳米片（GNSs）添加到Sn-58Bi低温钎料中，研究了GNSs对钎料熔化温度、润湿性能、剪切强度、显微组织和界面反应的影响。结果表明：添加GNSs可以改善Sn-58Bi钎料焊点的润湿性能和抗剪切强度，但对其熔化温度的影响较小。随着GNSs的添加，钎料得到了相对细化的显微组织，界面金属间化合物（IMC）的厚度明显降低，并逐渐趋于平整。另外，随着GNSs的加入，Sn-58Bi钎料的剪切断裂模式从脆性断裂转变为脆性和韧性混合的断裂模式，这与其抗剪切强度的变化是一致的。因此，添加微量的GNSs是增强Sn-58Bi/Cu焊点可靠性的有效途径。

关键词：石墨烯纳米片；显微组织；润湿性；剪切强度；可靠性

作者简介：姜　楠，男，1996年生，硕士生，江苏师范大学机电工程学院，江苏 徐州 221116，E-mail：jiangnan2972@163.com